Disruption of PPARγ/β-catenin–mediated regulation of apelin impairs BMP-induced mouse and human pulmonary arterial EC survival

Tero-Pekka Alastalo,[1] Molong Li,[1] Vinicio de Jesus Perez,[2] David Pham,[1] Hirofumi Sawada,[1] Jordon K. Wang,[3,4] Minna Koskenvuo,[1] Lingli Wang,[1] Bruce A. Freeman,[5] Howard Y. Chang,[3,4] and Marlene Rabinovitch[1]

[1]Department of Pediatrics, [2]Department of Medicine, [3]Program in Epithelial Biology, and [4]Program in Cancer Biology, Stanford University, Stanford, California, USA. [5]Department of Pharmacology and Chemical Biology, University of Pittsburgh, Pittsburgh, Pennsylvania, USA.

Reduced bone morphogenetic protein receptor 2 (BMPR2) expression in patients with pulmonary arterial hypertension (PAH) can impair pulmonary arterial EC (PAEC) function. This can adversely affect EC survival and promote SMC proliferation. We hypothesized that interventions to normalize expression of genes that are targets of BMPR2 signaling could restore PAEC function and prevent or reverse PAH. Here we have characterized, in human PAECs, a BMPR2-mediated transcriptional complex between PPARγ and β-catenin and shown that disruption of this complex impaired BMP-mediated PAEC survival. Using whole genome-wide ChIP-Chip promoter analysis and gene expression microarrays, we delineated PPARγ/β-catenin–dependent transcription of target genes including *APLN*, which encodes apelin. We documented reduced PAEC expression of apelin in PAH patients versus controls. In cell culture experiments, we showed that apelin-deficient PAECs were prone to apoptosis and promoted pulmonary arterial SMC (PASMC) proliferation. Conversely, we established that apelin, like BMPR2 ligands, suppressed proliferation and induced apoptosis of PASMCs. Consistent with these functions, administration of apelin reversed PAH in mice with reduced production of apelin resulting from deletion of PPARγ in ECs. Taken together, our findings suggest that apelin could be effective in treating PAH by rescuing BMPR2 and PAEC dysfunction.

Introduction

Pulmonary arterial hypertension (PAH) is characterized by a progressive increase in pulmonary vascular resistance (PVR) that culminates in right-sided heart failure. There is no cure for this condition, and the mainstays of therapy include primarily vasodilators that may improve symptoms and survival for a limited time. For many patients, lung transplantation is eventually necessary, with its inherent high morbidity and mortality. Histologically, advanced PAH is characterized by loss of the microcirculation as a result of EC apoptosis, abnormal muscularization of precapillary arterioles, and neointimal occlusive changes in larger intra-acinar vessels. These occlusive changes are caused by proliferation of cells with characteristics of SMCs, accumulation of extracellular matrix, inflammation, and fibrosis. In some cases, plexiform lesions are observed, in which the lumen and adventitia of the vessels are filled with EC-lined channels. These represent ECs that are resistant to apoptosis and poorly differentiated (1).

Numerous studies have tried to link the pathobiology of these changes to mutations or dysfunction of bone morphogenetic protein receptor 2 (*BMPR2*). In 25% of sporadic and up to 80% of the familial form of idiopathic PAH (IPAH), there are germline mutations in the reading frame of *BMPR2* (2, 3). Moreover, reduced expression of BMPR2 is observed in patients without mutations and in PAH that is associated with other primary conditions (4, 5).

Conflict of interest: Bruce A. Freeman declares a financial interest in Complexa Inc.
Citation for this article: *J Clin Invest.* 2011;121(9):3735–3746. doi:10.1172/JCI43382.

Both PASMC and EC dysfunction have been linked to impaired BMPR2 signaling in the pathogenesis of PAH (6–9). Loss of BMPR2 signaling promotes EC apoptosis, and reduced EC survival can underlie the loss of microvessels both in the clinical setting and in animal models of PAH. Furthermore, decreased BMPR2 expression leads to attenuation of the angiogenic capacity of PAECs (9). These observations are in keeping with other studies showing BMPs to be potent regulators of EC function (10). Our recent study in PAECs has shown that BMPR2-mediated signaling recruits the Wnt/β-catenin pathway to mediate expression of genes that promote PAEC homeostasis (9).

Further support for EC dysfunction in the pathogenesis of PAH has come from studies in transgenic mice with conditional heterozygous or homozygous deletion of *BMPR2* in pulmonary ECs using an *ALK1* promoter–driven Cre (11). In addition to mutations in *BMPR2*, predisposition to PAH has also been associated with mutations in other TGF-β superfamily receptors, *ALK1* or *ENG*, that are primarily expressed in ECs (12).

In contrast to PAECs, BMPs exert antiproliferative and proapoptotic actions in PASMCs (6, 7) via PPARγ-regulated mechanisms (13). Decreased PPARγ expression is observed in vascular lesions in human PAH patients (14). Conditional deletion of PPARγ both in SMCs (13) and in ECs (15) produces PAH, affirming a central role for this nuclear receptor in PAH-related gene expression.

In this study, the link between BMPR2 signaling and PPARγ-dependent gene expression was investigated to identify target genes critical for EC homeostasis. We showed that BMP-2–mediated

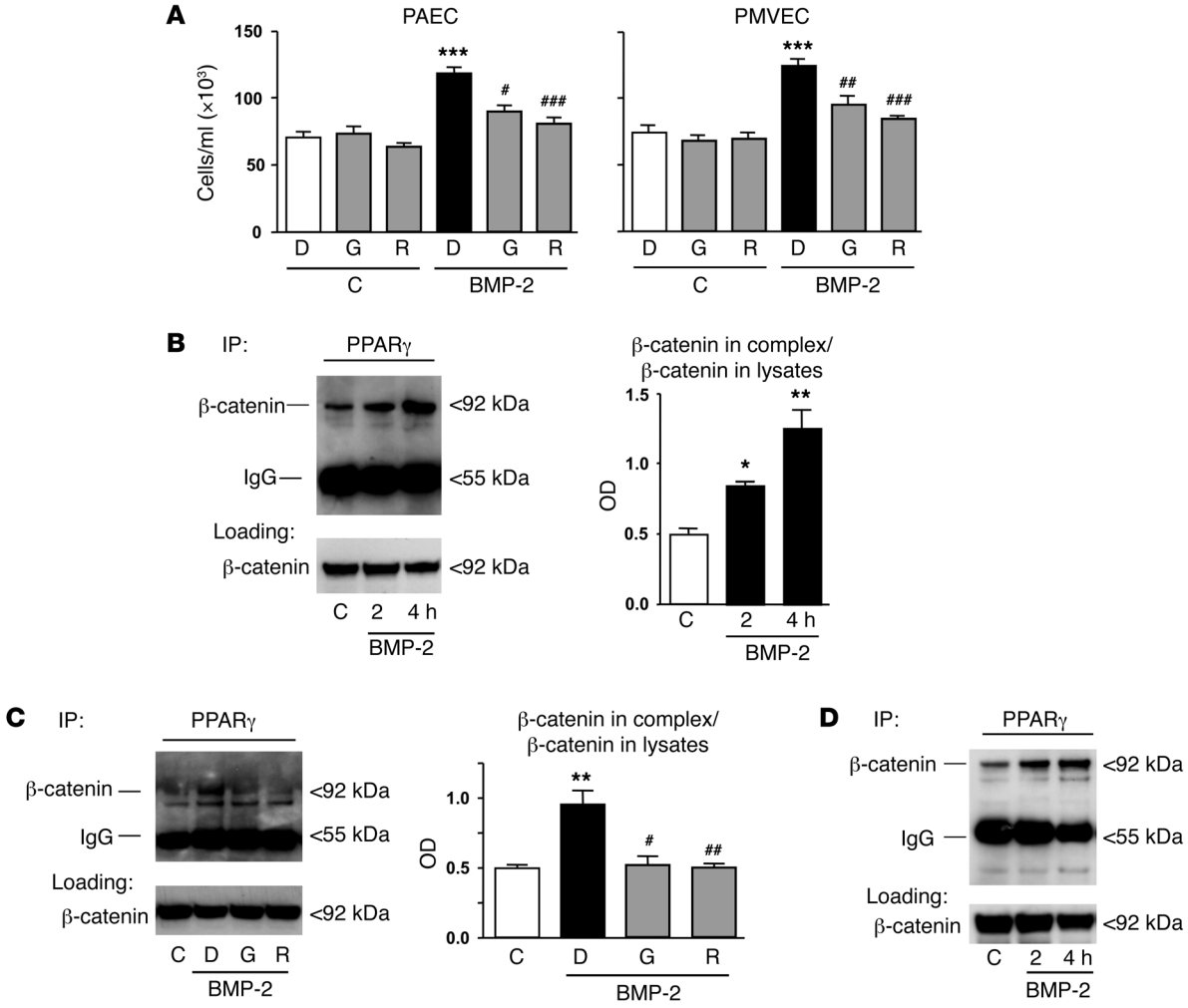

Figure 1

PPARγ ligands abrogate BMP-2–mediated survival and inhibit BMP-2–mediated interaction between PPARγ and β-catenin in PAECs. (**A**) Cell counts were used to determine PAEC and PMVEC survival after 24 hours under serum-free (SF) conditions. Equal numbers of cells were pretreated for 1 hour with DMSO (D; 1:10,000), GW9662 (G; 1 μM), or rosiglitazone (R; 1 μM) before stimulation with vehicle control (C) or BMP-2 (10 ng/ml). Bars represent mean ± SEM from 3 separate experiments with 3 replicates per condition. (**B**) Western immunoblot and densitometric analysis of β-catenin levels after IP with the PPARγ Ab in response to BMP-2. (**C**) Western immunoblot of β-catenin IP with PPARγ Ab under conditions in **A**. (**D**) β-catenin in nuclear extracts after IP with PPARγ Ab. In **B**–**D**, loading control shows β-catenin in lysates before IP. Bars represent mean ± SEM from 3 separate experiments. $^{*}P < 0.05$, $^{**}P < 0.01$, $^{***}P < 0.001$ vs. control; $^{\#}P < 0.05$, $^{\#\#}P < 0.01$, $^{\#\#\#}P < 0.001$ vs. DMSO; 1-way ANOVA with Bonferroni multiple comparison test.

EC survival was dependent upon formation of a nuclear complex between PPARγ and β-catenin that was inhibited by synthetic — but not endogenous — PPARγ ligands, such as nitroalkene derivatives of unsaturated fatty acids (NO_2-FAs). By using ChIP coupled with DNA microarray analyses in combination with gene expression microarrays, apelin was identified as a transcriptional target of the PPARγ/β-catenin complex that displays reduced expression in ECs of IPAH patients with deficient BMPR2 expression. Notably, siRNA-induced reduction of apelin levels in PAECs impaired PAEC survival and promoted PASMC proliferation. Furthermore, apelin directly suppressed SMC proliferation in response to growth factors and was proapoptotic. Consistent with these observations, the PAH and related arterial muscularization of *TIE2CrePPARγ*$^{fl/fl}$ mice, in which apelin is reduced, was reversed by a 2-week administration of apelin.

Results

To investigate the role of PPARγ in BMP-2–mediated EC survival, human central PAECs or pulmonary microvascular ECs (PMVECs) were pretreated with the PPARγ antagonist GW9662 or the agonist rosiglitazone for 1 hour prior to BMP-2 stimulation. Surprisingly, both these ligands abrogated the BMP-2–mediated survival response (Figure 1A). As GW9662 also displays PPARγ agonist activity (16, 17), i.e., antiproliferative (18) and antidiabetic (19) effects in murine models of disease, we subsequently evaluated endogenously generated NO_2-FAs that act as covalently reacting partial PPARγ agonists (20).

In PAECs, β-catenin regulates genes necessary for BMP-2–mediated survival (9), and in cancer cells, β-catenin interacts with PPARγ (21, 22). Co-IP with whole cell extracts showed a complex between PPARγ and β-catenin in PAECs (Figure 1B) and in

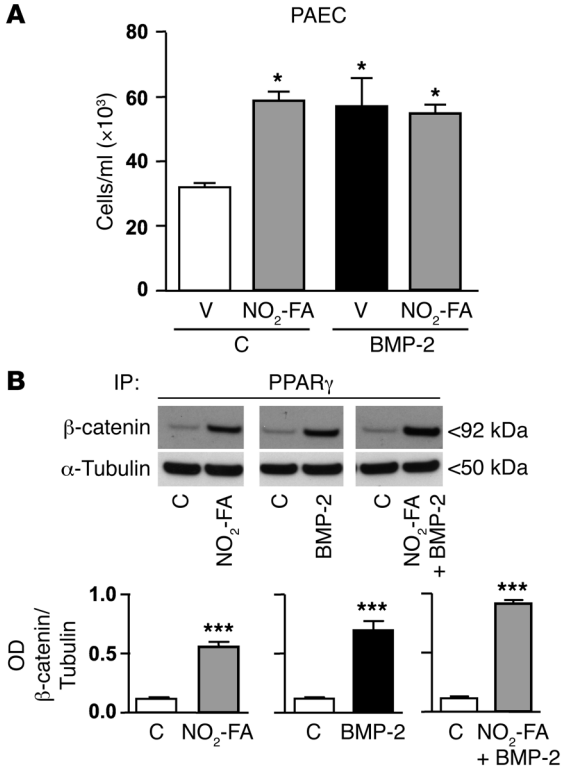

Figure 2

NO_2-FA promotion of survival and induction of PPARγ/β-catenin complex formation in PAECs. (**A**) Cell counts were used to determine PAEC survival after 24 hours under SF conditions. Equal numbers of cells were pretreated for 1 hour with 1 μM NO_2-FA or methanol as vehicle (V) before stimulation with BMP-2 (10 ng/ml) or water as control. Bars represent mean ± SEM from 3 separate experiments with 3 replicates per condition. (**B**) Western immunoblot and densitometric analysis of β-catenin levels after IP with PPARγ Ab in response to NO_2-FA, BMP-2, or the combination. Loading control with α-tubulin showed equal loading of protein lysate before IP reaction. Bars represent mean ± SEM from 3 separate experiments. $^*P < 0.05$, $^{***}P < 0.001$ vs. control, 1-way ANOVA with Bonferroni multiple comparison test (**A**) or unpaired 2-tailed *t* test (**B**).

PMVECs (data not shown). Formation of this complex increased 2- to 3-fold after BMP-2 stimulation (Figure 1B). Nonimmune IgG showed that co-IP required anti-PPARγ (Supplemental Figure 1; supplemental material available online with this article; doi:10.1172/JCI43382DS1). The BMP-2–mediated formation of PPARγ/β-catenin complexes was attenuated by both synthetic PPARγ ligands, GW9662 and rosiglitazone (Figure 1C), consistent with their similar effect on survival. Co-IP with nuclear extracts indicated that BMP-2 could be inducing the formation of the PPARγ/β-catenin complex in the nuclei of PAECs (Figure 1D), as previously described and suggested by our confocal microscopy observations (ref. 23 and data not shown). As a positive control, we carried out similar experiments using NO_2-FAs as more naturally occurring PPARγ agonists. The NO_2-FA species 10-nitro-octadeca-9-enoic acid promoted PAEC survival to the same extent as did BMP-2 and did not interfere with or increase BMP-2–mediated PAEC survival (Figure 2A). Furthermore, this NO_2-FA induced a complex between PPARγ and β-catenin that was not disrupted when NO_2-FA was used together with BMP-2 (Figure 2B).

Identifying apelin as a target of the PPARγ/β-catenin transcription factor complex by microarray strategies. To investigate the targets of transcription activated by the PPARγ/β-catenin complex in response to BMP-2 stimulation, we applied ChIP with PPARγ and β-catenin Abs coupled with DNA microarray analyses (referred to herein as ChIP-chip) using the Roche Nimblegen promoter tiling array (see Methods). With the PPARγ ChIP-chip, we identified 1,079 significant peaks (defined as false discovery rate [FDR] less than 0.20) in control PAECs and double that number (2,191) in the BMP-2–treated PAECs (Figure 3A). The β-catenin ChIP-chip revealed far fewer peaks in unstimulated cells and many more after BMP-2 treatment (267 vs. 6,018; Figure 3A). Interestingly, in the BMP-2–treated sample, β-catenin co-occupied 70% (1,543) of the promoters bound by PPARγ (Figure 3B), and PPARγ co-occupied 25% of the promoters bound by β-catenin. To analyze the distance between PPARγ and β-catenin bound regions on these co-occupied promoters, we used the peak coordinates obtained by NimbleScan to determine how far the center coordinates are from each other. There was a marked overlap between PPARγ and β-catenin bound regions on co-occupied promoters (Figure 3C). In fact, in 78% (1,202) of co-occupied promoters, the peaks were within 300 bp. We used this 300-bp distance as a threshold for selecting genes for further analysis.

To further refine the list of putative target genes that were not only co-occupied but also transcribed in response to BMP signaling, we silenced BMPR2 or β-catenin expression in PAECs using siRNA oligonucleotides as previously described (9) and studied changes in gene expression. We did not use stable or transient PPARγ siRNA, as we had only been only able to show a reduction in *PPARG* mRNA, not PPARγ protein. We isolated RNA from 2 independent PAEC cultures transfected with control, BMPR2, or β-catenin siRNA, and every RNA sample was hybridized on 2 separate arrays. The 4 hybridizations for each condition showed high reproducibility. Furthermore, as a methodological validation of the microarray analyses, we determined that BMPR2 and β-catenin were the most downregulated genes in the samples treated with their respective siRNAs.

Gene ontology analysis was carried out using genes in which loss of BMPR2 changed expression at least 1.5-fold and produced a *q* value less than 10% by Significance Analysis of Microarray (SAM). Our results revealed an important role for BMPR2 in PAEC biology. There was great enrichment for anatomical structure development, angiogenesis, vascular development, wound healing, and cell differentiation (Supplemental Table 1). Ontology analysis of genes with altered expression after reducing β-catenin yielded similar results. In addition, there was enrichment for cell proliferation, cell motility, and cell-matrix adhesion (Supplemental Table 2).

We then investigated which of the co-occupied ChIP-chip targets also showed significant changes in gene expression after both BMPR2 and β-catenin siRNA (at least 1.5-fold, $q < 20\%$, after loss of both BMPR2 and β-catenin). Using these criteria, we found 18 potential target genes (Table 1). A few, such as adrenomedullin-2 (*ADM2*; a homolog of adrenomedullin) (24), apelin (*APLN*) (25), *SOX18*, and vasohibin 1 (*VASH1*) (26), are recognized regulators of EC function, but others have not been well characterized. We assessed these and 4 other genes of interest implicated in angiogenesis by quantitative real-time PCR (qRT-PCR) and confirmed a change similar to that detected by the gene expression arrays (Supplemental Table 3 and Figure 4). Of the genes identified, *APLN* has been linked to both experimental models and clinical examples of PAH. Circulating ape-

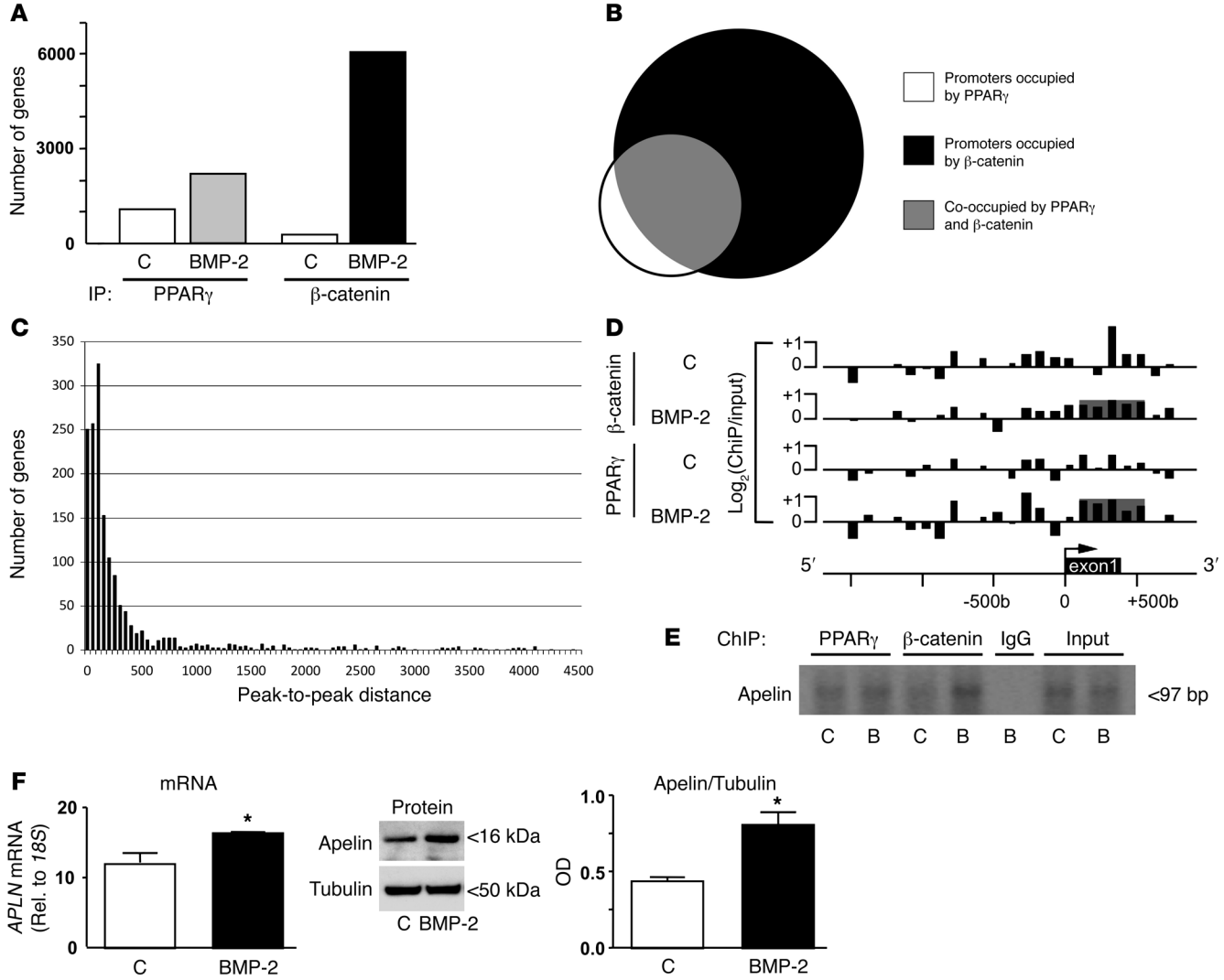

Figure 3

Microarray strategies reveal apelin as a target of BMP signaling and of the PPARγ/β-catenin complex. (**A**) Number of significant peaks (FDR < 0.20) in PPARγ and β-catenin ChIP-chip assays determined by NimbleScan in PAECs treated for 4 hours with vehicle control or BMP-2 (10 ng/ml). (**B**) Co-occupancy of β-catenin in PPARγ-bound promoter in BMP-2–treated samples. (**C**) Peak-to-peak analysis of co-occupied genes in BMP-2–treated samples. (**D**) Occupancy of PPARγ or β-catenin across approximately 2 kb of the *APLN* gene, as measured by ChIP-chip in vehicle control– and BMP-2–treated PAECs. The *y* axis plots the ratio of hybridization signals of ChIP over input genomic DNA in log2 space. Shaded gray region denotes significant peaks, as determined by NimbleScan. (**E**) ChIP-PCR with primers targeted against the ChIP-chip peak was performed for PPARγ, β-catenin, or IgG ChIPs with PAECs treated with vehicle control or BMP-2 (B). The PCR products were run on a 2% agarose gel. Input samples were used as a positive control. (**F**) PAECs were stimulated for 8 hours with vehicle control or BMP-2 (10 ng/ml), and expression of *APLN* mRNA and apelin protein was analyzed. Bars represent mean ± SEM from 3 separate experiments. **P* < 0.05, unpaired 2-tailed *t* test.

lin levels are decreased in IPAH patients (27), and apelin administration improves RV function in the monocrotaline rat model of PAH (28). In addition, loss of apelin worsens hypoxia-induced pulmonary hypertension in association with decreased number and enhanced muscularization of peripheral arteries (29).

ChIP-chip analysis of BMP-2–treated PAECs showed significant and overlapping binding of both PPARγ and β-catenin to a site spanning the first exon and first intron of the *APLN* gene +102 to +552 nucleotides downstream of the transcription start site (Figure 3D). This region contains a potential PPARγ response element (PPRE). ChIP-PCR analysis showed stronger *APLN* DNA binding in BMP-2–treated samples, particularly in those subjected to IP with the β-catenin Ab (Figure 3E). These findings were consistent with a BMP-2–mediated increase in *APLN* mRNA and apelin protein (Figure 3F). The greater increase in protein relative to mRNA may reflect an increase in translation of a relatively unstable mRNA. On Western immunoblots, we detected mainly a 16-kDa apelin dimer, the major form of apelin found in tissues and cells (30). Furthermore, expression of the 16-kDa protein correlated with the level of *APLN* mRNA, and apelin siRNA significantly decreased its expression (see below).

To further relate apelin expression to the BMPR2/PPARγ/β-catenin signaling axis, we repeated silencing of BMPR2 and β-catenin in PAECs and observed a 50%–75% decrease in *APLN* mRNA and apelin protein (Figure 5, A and B). We then assessed

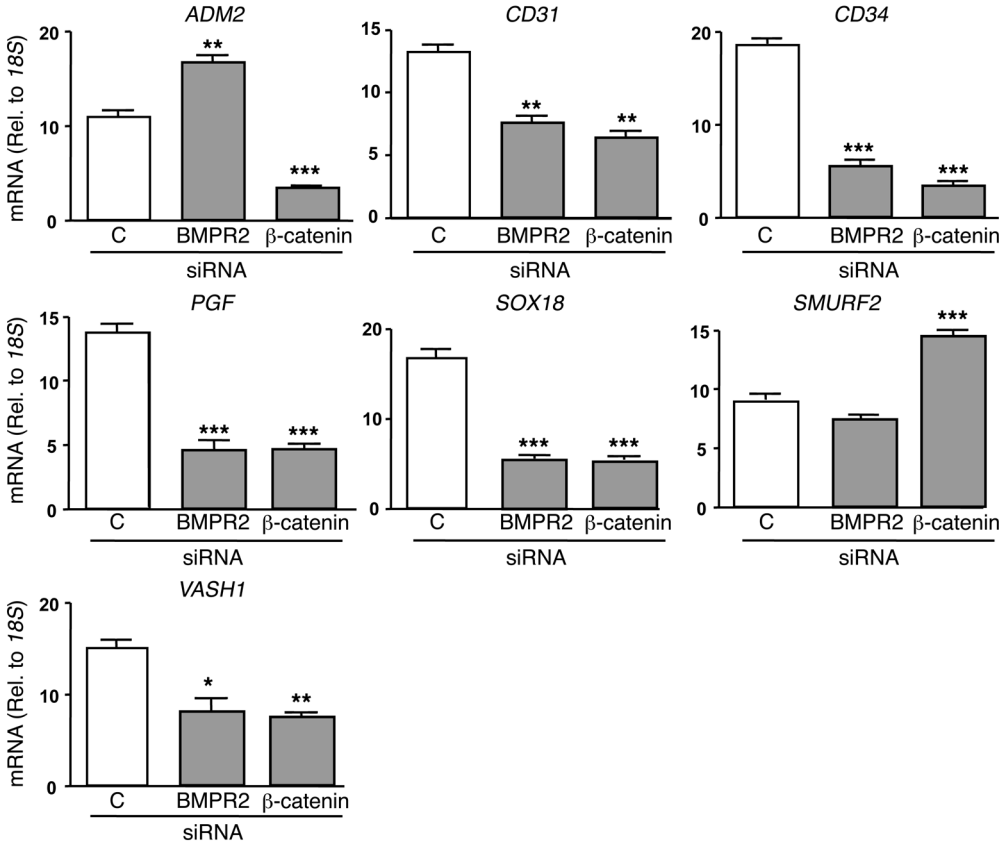

Figure 4
Confirmation of gene expression changes suggested by microarray. Of the genes listed in Supplemental Table 3, we selected 7 for qRT-PCR. Bars represent mean ± SEM from 3 separate experiments. *$P < 0.05$, **$P < 0.01$, ***$P < 0.001$ vs. control siRNA, 1-way ANOVA with Bonferroni multiple comparison test.

mRNA and protein expression in whole lung extracts and in PMVECs of mice with deletion of *PPARγ* in ECs (*TIE2CrePPARγ$^{fl/fl}$* mice; ref. 15). A greater than 50% reduction in apelin protein was observed in lungs of *TIE2CrePPARγ$^{fl/fl}$* mice (Figure 5C), and a similar reduction in *Apln* mRNA and apelin protein was found in PMVECs isolated from these mice (Figure 5, D and E).

Apelin expression is decreased in pulmonary ECs of IPAH patients. Dysfunctional BMP signaling and decreased circulating apelin levels are associated with IPAH (27). However, it is uncertain whether this reflects reduced apelin expression in the pulmonary vasculature of IPAH patients. Immunhistochemical (IHC) analysis of apelin expression using preincubation with the apelin peptide to control for specificity of immunoreactive sites revealed marked reduction in apelin in the pulmonary arterial endothelium of IPAH versus unused-donor control lungs (Figure 6A). To further pursue this observation, we used anti-human CD31–coated magnetic beads to isolate and culture PMVECs from IPAH and unused-donor control lungs. In these passage 2 EC cultures, the protein level of BMPR2 was reduced greater than 75% in IPAH patients (Figure 6B). Consistent with IHC-based observations, *APLN* mRNA and apelin protein levels were reduced by about 75% and 50%, respectively, in PMVECs from IPAH patients versus control unused-donor lungs (Figure 6, C and D).

Apelin is a prosurvival factor for pulmonary ECs. Apelin promotes systemic EC proliferation, migration, and angiogenesis, as reviewed by Sorli (31), but its role in EC survival has not been reported. We showed that administration of 100 nM apelin promoted survival by significantly reducing apoptosis of PAECs after serum starvation for 24 hours (as judged by caspase 3/7 activity, cell counts, and MTT assays; Figure 7, A and B). However, the protective effect of apelin was weaker than that of 50 ng/ml VEGFA, used as a positive control. We then showed that incubation with apelin also promoted survival of PMVECs harvested from both control and IPAH patient lungs (Figure 7C). Subsequent assays showed that apelin was also a proproliferative and promigratory factor in PAECs, as judged by cell count and the MTT assay and by Boyden chamber assay, respectively (Supplemental Figure 3, A–C).

Conversely, PAECs made deficient in apelin by siRNA — as judged by a 75% decrease in *APLN* mRNA and a 60% reduction in protein (Supplemental Figure 2) — underwent increased apoptosis under serum-free conditions for 12 and 24 hours compared with control siRNA–transfected PAECs, as assessed both by caspase 3/7 activity and by cell counts (Figure 5, D and E). PAECs made deficient in apelin by siRNA showed suppressed proliferation in response to 5% FBS and 50 ng/ml VEGFA as well as reduced migration with VEGFA (Supplemental Figure 3, B and C).

Apelin inhibits proliferation and is proapoptotic in PASMCs. We next showed that apelin produced by PAECs had a paracrine effect in inhibiting PASMC growth. That is, when conditioned medium harvested from PAECs deficient in apelin was applied to PASMCs,

Table 1
Co-occupied PPARγ/β-catenin targets with significant change in gene expression after loss of BMPR2 or β-catenin

Gene	Definition	BMPR2 loss		β-catenin loss	
		log_2	*q*	log_2	*q*
ADM2	Adrenomedullin 2	0.81	1.52%	–1.02	2.48%
ANKRD47	Ankyrin repeat domain 47	–1.12	20.51%	–0.71	9.71%
APLN	Apelin	–1.27	4.61%	–2.60	0.94%
BARD1	BRCA1 associated RING domain 1	0.85	7.94%	0.76	0.77%
E2F7	E2F transcription factor 7	1.12	3.07%	–0.82	9.71%
FAM89A	Family with sequence similarity 89, member A	–1.54	4.61%	–1.06	2.48%
HOMER1	Homer homolog 1	1.57	12.61%	1.23	6.41%
KDELC2	KDEL containing 2	0.69	1.52%	–1.97	0%
MMP28	Matrix metallopeptidase 28	–2.31	12.61%	–0.84	9.71%
MRAS	Muscle RAS oncogene	–0.85	20.51%	–1.06	14.37%
PLEKHG1	Pleckstrin homology domain containing family G member 1	–0.87	6.72%	–2.79	0.94%
PNMA2	Paraneoplastic antigen MA2	0.88	20.51%	–1.54	9.71%
SOX18	SRY-box containing gene 18	–1.41	6.72%	–1.53	1.89%
SS18L1	Synovial sarcoma translocation gene on chromosome 18-like 1	1.05	20.51%	1.26	3.45%
STAMBPL1	STAM binding protein-like 1	1.69	6.72%	1.34	6.41%
TAF5L	TAF5L-like RNA polymerase II	1.10	7.95%	0.61	9.71%
VASH1	Vasohibin 1	–0.81	12.61%	–1.14	1.89%
VPS53	Vacuolar protein sorting 53 homolog	1.81	20.51%	1.15	14.37%

Change in gene expression after silencing BMPR2 or β-catenin, relative to control siRNA, is shown as log_2 space. Significance of the expression change, as assessed by SAM, is shown as the *q* value for each siRNA condition.

a heightened proliferative response was apparent compared with either conditioned media from PAECs treated with control siRNA or even with 5% FBS, as assessed by cell counts and the MTT assay (Figure 8A). To confirm that the reduced apelin in the conditioned media of apelin siRNA–treated PAECs accounts for this response, we showed that 100 nM apelin directly attenuated PASMC proliferation in response to PDGFB (Figure 8B). In the absence of PDGFB, we noted that administration of apelin reduced the number of PASMCs below baseline and also resulted in a significant decrease in MTT level. This was consistent with the proapoptotic property of 10 and 100 nM apelin, as judged by the caspase 3/7 assay (Figure 8C).

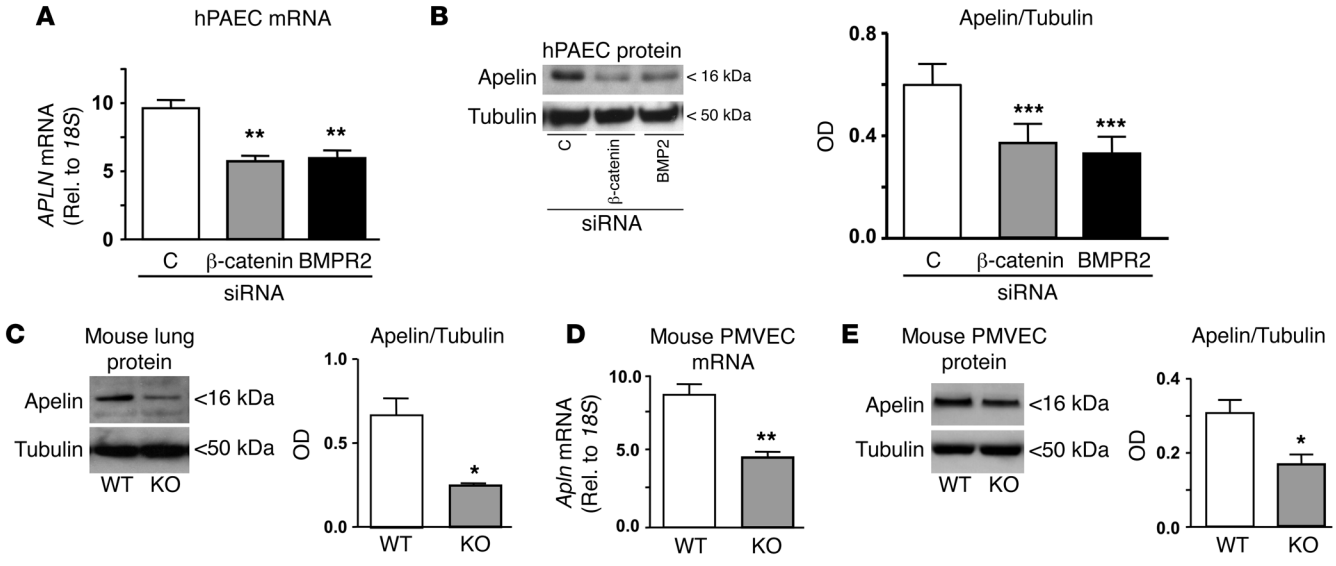

Figure 5
Loss of BMPR2, PPARγ, or β-catenin leads to decreased apelin expression. Levels of (**A**) *APLN* mRNA and (**B**) apelin protein after silencing BMPR2 or β-catenin with siRNA. Bars represent mean ± SEM from 3 separate experiments. (**C**) Apelin protein levels in lungs from WT and *TIE2CrePPARγ*$^{fl/fl}$ (KO) mice. Bars represent mean ± SEM from 3 separate animals per group. (**D**) *Apln* mRNA levels in mouse PMVECs at passage 1. Bars represents mean ± SEM in PMVECs harvested from 4 animals per group. (**E**) Apelin protein levels in mouse WT and *TIE2CrePPARγ*$^{fl/fl}$ PMVECs. Bars represent mean ± SEM from PMVEC cultures harvested from 4 different animals. **P* < 0.05, ***P* < 0.01, ****P* < 0.001 vs. respective control, 1-way ANOVA with Bonferroni multiple comparison test (**A** and **B**) or unpaired 2-tailed *t* test (**C**–**E**).

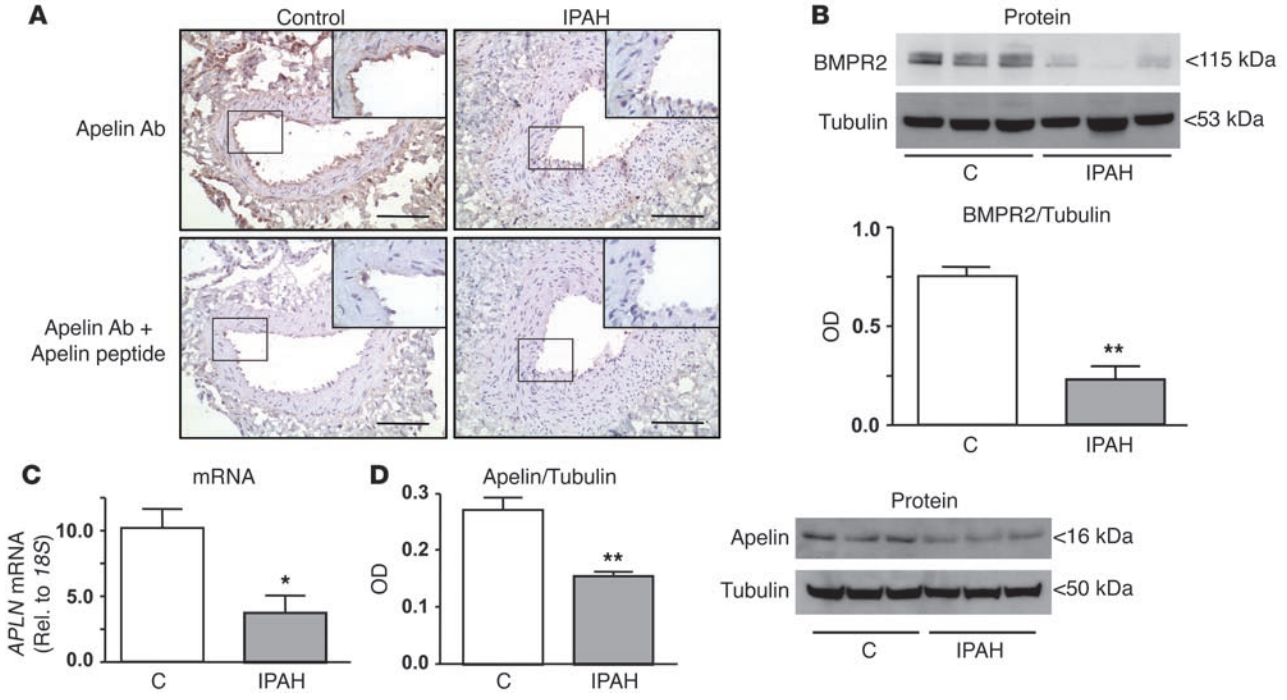

Figure 6
Decreased apelin expression in the endothelium of IPAH patients. (**A**) IHC in serial lung tissue sections from representative unused-donor control and IPAH patient lungs stained with Abs against apelin. Preincubation of Ab with apelin peptide was used as a specificity control. Higher-magnification endothelium in insets demonstrates greater apelin immunoreactivity in the control vessel. Scale bars: 100 μm. Original magnification, x200 (insets, ×630). (**B**) BMPR2 protein levels in PMVECs from control and IPAH patients. (**C**) *APLN* mRNA and (**D**) apelin protein expression in PMVECs from **B**. (**B**–**D**) Bars represent mean ± SEM from PMVECs isolated from 3 different patients per group. $^*P < 0.05$, $^{**}P < 0.01$ vs. control, unpaired 2-tailed *t* test.

Apelin treatment reverses PAH in TIE2CrePPARγ$^{fl/fl}$ mice. The *TIE2CrePPARγ$^{fl/fl}$* mouse has mild PAH, as previously reported by our group based on elevated RV systolic pressure (RVSP), RV hypertrophy (RVH), and muscularization of distal arteries (15). As expected for a downstream target of PPARγ, we documented reduced *Apln* mRNA and apelin protein expression in the lungs and PAECs of *TIE2CrePPARγ$^{fl/fl}$* mice versus their littermate controls (Figure 5, C–E). We then treated these mice with daily i.p. injections of 200 μg/kg apelin or PBS vehicle for 14 days. As shown in Figure 9, A–D, we observed reversal of RVSP, RVH, and muscularization of alveolar wall pulmonary arteries in *TIE2CrePPARγ$^{fl/fl}$* mice to values observed in littermate controls. Analysis of LV ejection fraction, LV shortening fraction, heart rate, and cardiac output showed no differences between the groups (Supplemental Figure 4).

Discussion

While dysfunctional BMP signaling is linked to the pathogenesis of IPAH, our present findings identified apelin as a secreted protein downstream of BMP signaling that regulates pulmonary vascular homeostasis. We showed that BMP-mediated expression of apelin was regulated by formation of a transcriptional complex between PPARγ and β-catenin and that this complex was induced by endogenous PPARγ ligands, such as NO_2-FAs. BMP-mediated apelin production contributed to EC homeostasis by promoting PAEC survival, proliferation, and migration. These features are functionally significant in the preservation and regeneration of the vasculature in response to injury. In addition to the autocrine functions of apelin, it displays a paracrine effect by attenuating the response of PASMCs to growth factors and by promoting apoptosis. These findings support the beneficial effect of apelin on cardiac function in rats with PAH (28), underscore the adverse impact of its loss on the severity of PAH (29), and make apelin an attractive pharmacological target for the treatment of PAH.

Our observation that the PPARγ antagonist GW9662 as well as the agonist rosiglitazone impaired BMP-2–mediated survival of PAECs or PMVECs was consistent with previous studies showing that these reagents can both induce anomalous PPARγ activation (19, 32). These observations reinforce current doubt as to how well this class of PPARγ-targeted drugs act as physiological regulators of PPARγ. The use of thiazolidinediones (TZDs), such as rosiglitazone, as antidiabetic drugs is under critical scrutiny, since it is becoming apparent that they are manifesting adverse side effects that include weight gain, fluid retention, hepatotoxicity, and risk of adverse cardiovascular events (33). This motivates consideration of whether the adverse effects of TZDs are related to their disruption of more salutary PPARγ-mediated gene regulation. At least one case report indicates an adverse effect of rosiglitazone on pulmonary hypertension in a patient with diabetes (34). Our studies suggest a need for more effective PPARγ-targeted drugs that have partial agonist properties that are more consistent with endogenous ligands. Endogenous ligands for PPARγ include NO and NO_2-FAs. These species show a very high affinity for activating PPARγ as partial agonists by covalently adducting the Cys285 of the ligand binding domain (16, 35–37). Our present studies demonstrated that NO_2-FAs were also

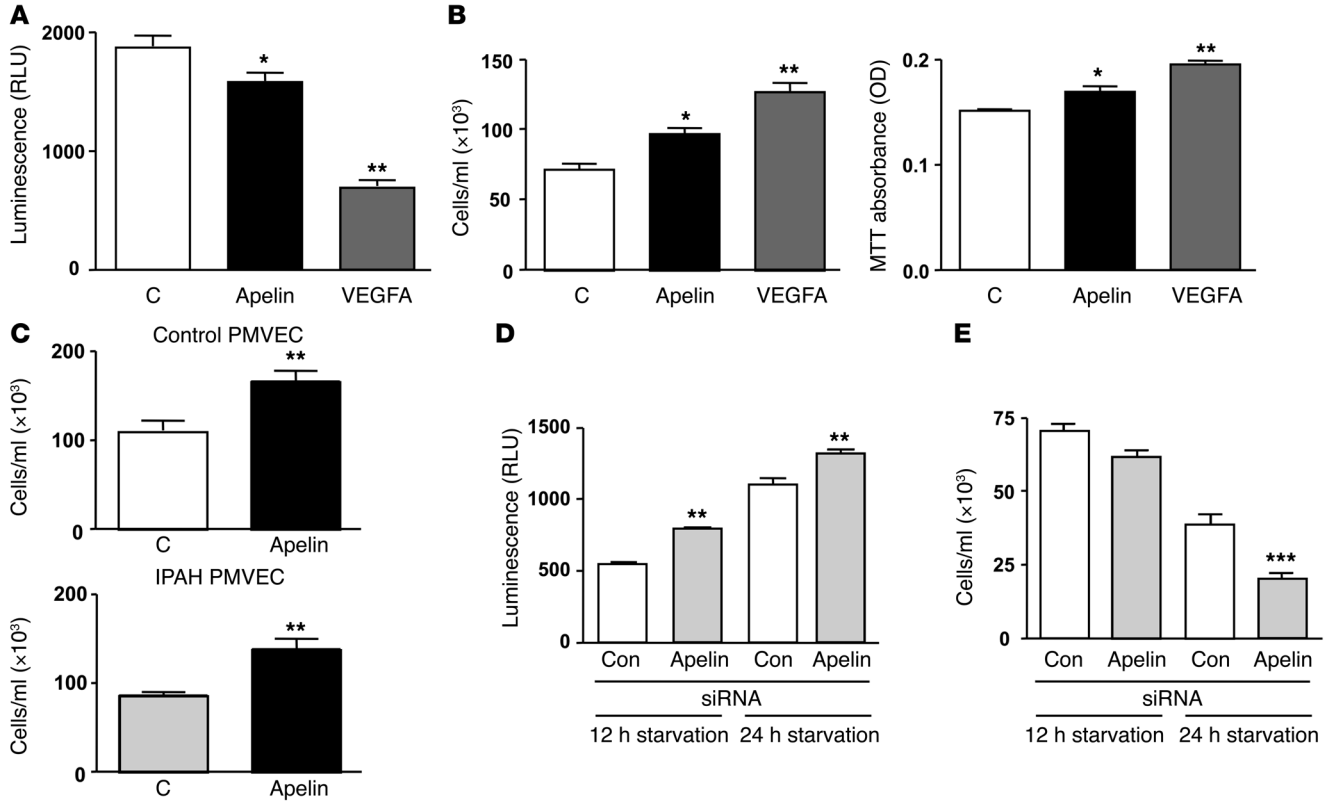

Figure 7

Apelin promotes PAEC survival. (**A**) Caspase 3/7 activity was used to measure the level of apoptosis in PAECs exposed for 24 hours to SF medium in the presence of vehicle control, apelin (100 nM), or VEGFA (50 ng/ml). (**B**) PAEC survival under these conditions was also determined by cell count and MTT analyses. (**C**) Survival in the presence of apelin was also assessed by cell counts in PMVECs isolated from control and IPAH patients. (**D**) Apoptosis level in control siRNA– and apelin siRNA–treated PAECs, as determined by caspase 3/7 assay under SF conditions. (**E**) Survival of apelin-deficient PAECs was determined by cell count after 24 hours of exposure to SF conditions. Baseline represents cell number before switching to SF medium. Bars represent mean ± SEM from 3 separate experiments with 6 replicates per condition in **A** and **D** and 3 replicates per condition in **B**, **C**, and **E**. $^{*}P < 0.05$, $^{**}P < 0.01$, $^{***}P < 0.001$ vs. respective control, 1-way ANOVA with Bonferroni multiple comparison test.

distinguished from TZD PPARγ agonists, such as rosiglitazone, by not disrupting the interaction of PPARγ with β-catenin (9). Moreover, NO_2-FAs were capable of inducing PPARγ/β-catenin complex formation independent of exogenous BMP stimulation, consistent with their overall promotion of PAEC survival.

Our group previously described BMP-mediated regulation of PPARγ in PASMCs (13), but in these studies, β-catenin is only transiently transcriptionally active (38). Moreover, rosiglitazone functioned like BMP-2 in repressing proliferation of SMCs in response to growth factors. Previous cancer cell studies (21, 22) indicated a physical interaction between PPARγ and β-catenin that was attributed to PPARγ-mediated translocation of β-catenin to the cytosol for proteasomal degradation (22). Notably, one report indicates that the PPARγ/β-catenin complex can bind a PPRE, and that β-catenin can promote transcription of a PPRE reporter (21). Association of β-catenin with several other nuclear receptors has been well documented, although the functional significance of these interactions was not well defined (39). We showed herein that interaction between PPARγ and β-catenin promoted regulation of genes that confer normal function and homeostasis to vascular cells. The mechanism promoting this interaction is not known, but our previous studies suggest that it is not pSmad dependent (9).

We carried out ChIP-chip and microarray analyses to determine which of the co-occupied genes are downstream of BMPR2-mediated signaling and have β-catenin–dependent expression. With the criteria used, we may have excluded a large number of gene targets of the PPARγ/β-catenin complex. Although we identified a number of genes related to EC homeostasis, we focused on *APLN* among the 18 targets, both because it was among the most highly regulated and because its reduction, like that of BMPR2, was linked to clinical PAH (28).

Apelin is highly expressed by systemic ECs, and a previous study showing that it can promote vascular regeneration (31) is in keeping with the downstream actions of BMPR2 signaling. We showed herein that decreased apelin expression in PAECs increased their susceptibility to apoptosis, an event that can augment microvascular injury and impair recovery. As decreased survival is also observed in ECs deficient in BMPR2 (8, 9), our observations suggest that this may be related to reduced levels of apelin, and thus might be prevented by apelin administration.

Paracrine effects of apelin were previously related to its activation of cardiac contractility (40) and vasodilatation, in part by inducing NO production (30, 41). Our coculture studies demonstrated that the apelin-deficient PAECs also promoted PASMC

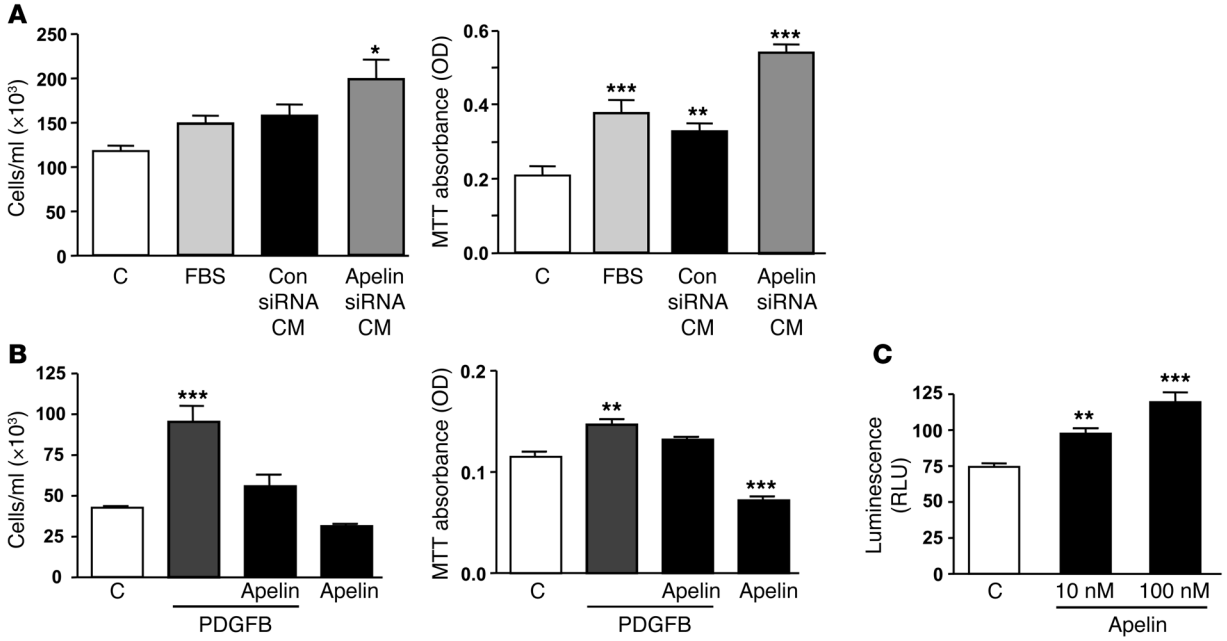

Figure 8

Apelin deficiency in PAECs contributes to PASMC proliferation. (**A**) PAEC-conditioned media (CM) after treatment with control or apelin siRNA (see Methods) was used to stimulate PASMCs for 72 hours, and proliferation was analyzed by cell counts and MTT assay. 5% FBS was used as a positive control, and starvation media alone was used as a baseline control. (**B**) Effect of 100 nM apelin on 20 ng/ml PDGFB–mediated PASMC proliferation, analyzed by cell counts and MTT assays at 72 hours. (**C**) Caspase 3/7 assay to measure apoptosis in PASMCs exposed to 10 or 100 nM apelin under SF conditions for 48 hours. Bars represent mean ± SEM from 3 separate experiments with 6 replicates per condition. $^{*}P < 0.05$, $^{**}P < 0.01$, $^{***}P < 0.001$ vs. respective baseline control, 1-way ANOVA with Bonferroni multiple comparison test.

proliferation, related either to reduced EC survival (42) or to active production of mediators of PASMC proliferation. We documented direct growth-suppressing effects of apelin on SMCs that were minimized in apelin-deficient EC–conditioned medium. Whereas previous studies suggested that apelin promotes systemic SMC proliferation (43), the opposite effect occurred in PASMCs. However, our study is consistent with a recent report indicating that apelin protects against atherosclerosis and that apelin treatment can inhibit angiotensin II–mediated neointimal formation (44).

Apelin is the only known ligand for the APJ receptor, and the APJ receptor can mediate the effects of apelin on the cardiovascular system. However, the phenotype of the apelin-KO mouse is far less severe that that of the APJ-KO mouse, which dies in embryonic life in association with cardiac defects (45), suggestive of additional APJ ligands or ligand-independent effects of the receptor. Apelin-deficient mice have decreased myocardial contractility under stress (45) and retardation of retinal angiogenesis (46), as well as exaggerated pulmonary hypertension (29). The latter has been attributed to the induction of eNOS by apelin. In those studies, as in ours, apelin can induce angiogenesis by interacting with VEGFA and serum factors such as FGF2, as well as via eNOS induction.

Although it was previously suggested, using a lacZ reporter transgenic mouse model (47), that apelin expression is restricted to ECs of capillaries and veins, our observations and those of others noted expression of apelin in precapillary arteries in human lungs and in other tissues (48). This could be related to additional apelin promoter elements not included in the lacZ reporter construct or to lack of sensitivity of lacZ staining. We attribute the reduced apelin in PAECs from patients with IPAH to their reduced BMPR2 expression.

Since loss of BMPR2 in ECs is lethal in the embryo, we chose to test whether the PAH observed in mice as a consequence of *PPARγ* deletion in ECs and reduced apelin production could be reversed by adding back exogenous apelin. In the *TIE2CrePPARγ*$^{fl/fl}$ mouse, the manifestation of apelin loss is the absence of its paracrine effect in suppressing SMC proliferation and muscularization of distal arteries. Adding exogenous apelin was sufficient to reverse this morphological change and the associated mild PAH and RVH and was in keeping with the studies in cultured PAECs showing that apelin induced SMC apoptosis. It would be of interest to test whether apelin is reduced in other models of PAH and whether it also promotes regeneration of lost microvessels associated with PAH.

Current experimental approaches to reverse pulmonary vascular remodeling and treat PAH have focused either on promoting SMC apoptosis (49) or on inducing regeneration of precapillary arteries (50). Some of these approaches are already finding their way into clinical trials. Our observations in the present study suggest that apelin can do both. Moreover, it represents the replacement of a key downstream gene that is lost when there is dysfunctional BMPR2 signaling. This, coupled with its properties as a vasodilator and as a potent activator of LV and RV contractility (28, 51), makes apelin a very attractive therapeutic target for treating PAH.

Methods

Further information can be found in Supplemental Methods.

Cell culture. PAECs (ScienCell) and human and mouse PMVECs were grown in commercial EC media (Sciencell). Cells were subcultured at a 1:6 ratio in gelatin-coated dishes (BD Falcon and Corning) and used at passages 4–8.

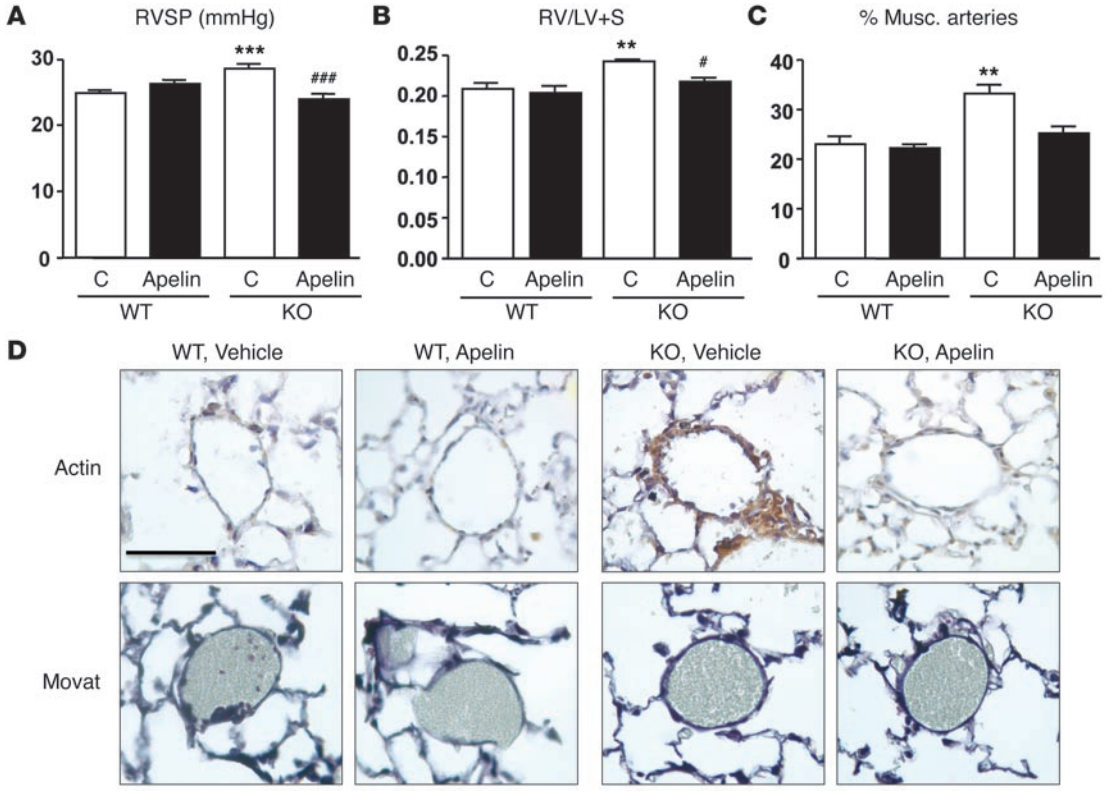

Figure 9

Apelin replacement reverses PAH in *TIE2CrePPARγ*$^{fl/fl}$ mice. (**A**) RV systolic pressure (RVSP) measurement of WT or *TIE2CrePPARγ*$^{fl/fl}$ mice treated with PBS vehicle control or apelin (200 μg/kg). (**B**) RV mass, measured as a ratio of the RV to that of the LV plus septum (RV/LV+S). (**C**) Muscularization of alveolar wall arteries is shown as a percentage of muscularized arteries from all 15- to 50-μm-diameter arteries. Bars represent mean ± SEM from 7 (**A** and **B**) or 5 (**C**) animals per group. (**D**) Representative anti–αSMC-actin (Actin) and Movat pentachrome–stained sections of pulmonary arteries, demonstrating reduced muscularization of pulmonary arteries in apelin-treated *TIE2CrePPARγ*$^{fl/fl}$ mice. Scale bar: 50 μm. Original magnification, ×400. $^{**}P < 0.01$, $^{***}P < 0.001$ vs. WT control, $^{\#}P < 0.05$, $^{\#\#\#}P < 0.001$ vs. untreated *TIE2CrePPARγ*$^{fl/fl}$ control, 1-way ANOVA with Bonferroni multiple comparison test.

Western immunoblotting. Western immunoblotting was done as previously described (9).

Co-IP. Protein was harvested by scraping the cells in RIPA buffer; 300 μg protein was used for Co-IP, and 40 μg of the same lysate for the loading control. Nuclear Co-IP was done by using the Nuclear Co-IP Kit (Active Motif).

ChIP-chip assay. Promoter tiling arrays (385K 2-array system) were produced by Roche NimbleGen, and hybridization and analysis was carried out following the protocols provided by the manufacturer. Significant hybridization peaks (FDR < 0.20) were determined by NimbleScan (version 2.5; Roche NimbleGen). Array data are available at Gene Expression Omnibus (accession no. GSE29489; http://www.ncbi.nlm.nih.gov/geo/query/acc.cgi?acc=GSE29489).

RNAi. siRNAs were transfected into PAECs using Lipofectamine 2000 (Invitrogen) as described previously (52). Knockdown efficiency for β-catenin and BMPR2 has been previously determined (9). Apelin knockdown was determined by qRT-PCR and Western immunoblotting (Supplemental Figure 2).

Gene expression microarray analysis. mRNA was isolated from control, BMPR2, or β-catenin siRNA–treated PAECs for Illumina Human Ref-12 BeadChip (Illumina) whole-genome gene expression array analysis using a standard protocol by Illumina. Microarray data analysis was performed using SAM (53) with a 2-class unpaired approach to compare expression data between control nontargeting siRNA– and gene-targeting siRNA–treated groups. Functional annotations were performed using the program DAVID 2008 with the Gene Ontology Biological Process terms database (http://david.abcc.ncifcrf.gov/). Array data are available at Gene Expression Omnibus (accession no. GSE18956; http://www.ncbi.nlm.nih.gov/geo/query/acc.cgi?acc=GSE18956).

mRNA expression by qRT-PCR. Total RNA was extracted and purified from cells with the RNAeasy Kit (Qiagen), then reverse-transcribed using Superscript II (Invitrogen) per the manufacturer's instructions. Expression levels of selected genes were quantified using preverified Assays-on-Demand TaqMan primer/probe sets (Applied Biosystems) and normalized to ribosomal RNA *18S*.

IHC. Paraffin sections of lungs from patients with IPAH and unused-donor control lungs were obtained through the tissue center of the Cardiovascular Medical Education and Research Fund–Pulmonary Hypertension Breakthrough Initiative (CMREF-PHBI) Network.

Isolation of human and mouse PMVECs. Human and murine PMVECs were isolated from digested whole lung tissue using CD31 Ab–coated magnetic beads (Dynabeads; Invitrogen).

EC survival, proliferation, and migration assays. PAEC or PMVEC survival and proliferation were assessed by cell counts and MTT assays. Caspase 3/7 was used to detect apoptosis as previously shown (9). Cell migration was assessed by a modified Boyden chamber assay.

PAEC-PASMC coculture. PAECs were transfected with nontargeting or apelin siRNA as described above. After 24 hours of recovery, cells were washed 3 times and then starved in low-serum conditions overnight (0.5% FBS; 5 ml per 10-cm dish). This PAEC-conditioned media was then used to stimulate quiescent PASMCs for 72 hours. The same starvation media not exposed to PAECs was used as a negative control, and 5% FBS was applied as a positive control.

PASMC proliferation and apoptosis assays. Cell counts and MTT assays were used to evaluate cell proliferation as previously described (13). The caspase 3/7 assay was performed using the same conditions as in PAECs (see above).

Experimental design to test whether apelin reverses PAH in TIE2CrePPARγ$^{fl/fl}$ mice. The creation and phenotypic characterization of *TIE2CrePPARγ$^{fl/fl}$* mice has been previously described (15). 12- to 15-week-old WT and *TIE2CrePPARγ$^{fl/fl}$* mice were treated with daily i.p. injections with either PBS vehicle or apelin (200 μg/kg) for 14 days before evaluation of hemodynamics, RV hypertrophy, and morphometric analysis of the pulmonary vasculature.

Statistics. Values from multiple experiments are shown as mean ± SEM. Statistical significance was determined using 1-way ANOVA followed by Bonferroni multiple comparison test. When only 2 groups were compared, statistical differences were assessed with unpaired 2-tailed *t* test. A *P* value less than 0.05 was considered significant. The number of samples or animals in each group is indicated in the figure legends.

Study approval. The studies herein were approved by the appropriate Institutional Review Board on human subjects and IACUC at Stanford University. Human subjects were recruited by the PHBI and provided informed consent prior to their participation. Stanford University has a human research protection program (HRPP), established in accordance with the principles and standards of the Association for the Accreditation of Human Research Protection Programs, that is applicable to all clinical research studies. All key personnel responsible for the design and conduct of the study have completed the Stanford University training course "Use of Human Subjects in Research," based on materials provided by NIH, including a Course Introduction and modules on Stanford's Multiple Project Assurance, Roles and Responsibilities, Case Study, and an optional module on History.

Acknowledgments

This work was supported by Postdoctoral Fellowships from the Sigrid Juselius Foundation, Instrumentarium Foundation, Finnish Foundation for Cardiovascular Research, Finnish Cultural Foundation, Finnish Foundation for Pediatric Research, and the Academy of Finland (to T.-P. Alastalo); the Department of Pediatrics of Mie University Graduate School of Medicine, Japan (to H. Sawada); The Scleroderma Research Foundation and an Early Career Scientist award from the Howard Hughes Medical Institute (H.Y. Chang); and National Institutes of Health (NHLBI) grant R01-HL087118 (to M. Rabinovitch) and HL58115 and HL64937 (to B.A. Freeman), CMREF-PHBI grant UL1RR024986, and the Dwight and Vera Dunlevie Endowed Professorship (to M. Rabinovitch). Lung tissues from IPAH and control patients provided by CMREF-PHBI were procured at the Transplant Procurement Centers at Baylor, Stanford University, UCSD, and Vanderbilt University; deidentified patient data were obtained via the Data Coordinating Center at the University of Michigan.

Received for publication April 16, 2010, and accepted in revised form June 15, 2011.

Address correspondence to: Marlene Rabinovitch, Stanford University School of Medicine, 269 Campus Drive, Room 2245B, Stanford, California 94305-5162, USA. Phone: 650.723.8239; Fax: 650.723.6700; E-mail: marlener@stanford.edu.

Tero-Pekka Alastalo and Minna Koskenvuo's present address is: Helsinki Children's Hospital, University of Helsinki, Helsinki, Finland.

Hirofumi Sawada's present address is: Department of Pediatrics, Mie University Graduate School of Medicine, Mie, Japan.

1. Masri FA, et al. Hyperproliferative apoptosis-resistant endothelial cells in idiopathic pulmonary arterial hypertension. *Am J Physiol Lung Cell Mol Physiol*. 2007;293(3):L548–L554.
2. Deng Z, et al. Familial primary pulmonary hypertension (gene PPH1) is caused by mutations in the bone morphogenetic protein receptor-II gene. *Am J Hum Genet*. 2000;67(3):737–744.
3. Lane KB, et al. Heterozygous germline mutations in BMPR2, encoding a TGF-beta receptor, cause familial primary pulmonary hypertension. *Nat Genet*. 2000;26(1):81–84.
4. Du L, et al. Signaling molecules in nonfamilial pulmonary hypertension. *N Engl J Med*. 2003; 348(6):500–509.
5. Atkinson C, et al. Primary pulmonary hypertension is associated with reduced pulmonary vascular expression of type II bone morphogenetic protein receptor. *Circulation*. 2002;105(14):1672–1678.
6. Morrell NW, et al. Altered growth responses of pulmonary artery smooth muscle cells from patients with primary pulmonary hypertension to transforming growth factor-beta(1) and bone morphogenetic proteins. *Circulation*. 2001;104(7):790–795.
7. Zhang S, et al. Bone morphogenetic proteins induce apoptosis in human pulmonary vascular smooth muscle cells. *Am J Physiol Lung Cell Mol Physiol*. 2003;285(3):L740–L754.
8. Teichert-Kuliszewska K, et al. Bone morphogenetic protein receptor-2 signaling promotes pulmonary arterial endothelial cell survival: implications for loss-of-function mutations in the pathogenesis of pulmonary hypertension. *Circ Res*. 2006;98(2):209–217.
9. de Jesus Perez VA, et al. Bone morphogenetic protein 2 induces pulmonary angiogenesis via Wnt-beta-catenin and Wnt-RhoA-Rac1 pathways. *J Cell Biol*. 2009;184(1):83–99.
10. David L, Feige JJ, Bailly S. Emerging role of bone morphogenetic proteins in angiogenesis. *Cytokine Growth Factor Rev*. 2009;20(3):203–212.
11. Hong KH, et al. Genetic ablation of the BMPR2 gene in pulmonary endothelium is sufficient to predispose to pulmonary arterial hypertension. *Circulation*. 2008;118(7):722–730.
12. Harrison RE, et al. Molecular and functional analysis identifies ALK-1 as the predominant cause of pulmonary hypertension related to hereditary haemorrhagic telangiectasia. *J Med Genet*. 2003; 40(12):865–871.
13. Hansmann G, et al. An antiproliferative BMP-2/PPARgamma/apoE axis in human and murine SMCs and its role in pulmonary hypertension. *J Clin Invest*. 2008;118(5):1846–1857.
14. Ameshima S, et al. Peroxisome proliferator-activated receptor gamma (PPARgamma) expression is decreased in pulmonary hypertension and affects endothelial cell growth. *Circ Res*. 2003; 92(10):1162–1169.
15. Guignabert C, et al. Tie2-Mediated Loss of Peroxisome Proliferator-Activated Receptor-{gamma} in Mice Causes PDGF-Receptor {beta}-Dependant Pulmonary Arterial Muscularization. *Am J Physiol Lung Cell Mol Physiol*. 2009;297(6):L1082–L1090.
16. Schopfer FJ, et al. Nitrolinoleic acid: an endogenous peroxisome proliferator-activated receptor gamma ligand. *Proc Natl Acad Sci U S A*. 2005; 102(7):2340–2345.
17. Leesnitzer LM, et al. Functional consequences of cysteine modification in the ligand binding sites of peroxisome proliferator activated receptors by GW9662. *Biochemistry*. 2002;41(21):6640–6650.
18. Burton JD, Castillo ME, Goldenberg DM, Blumenthal RD. Peroxisome proliferator-activated receptor-gamma antagonists exhibit potent antiproliferative effects versus many hematopoietic and epithelial cancer cell lines. *Anticancer Drugs*. 2007;18(5):525–534.
19. Rieusset J, et al. A new selective peroxisome proliferator-activated receptor gamma antagonist with antiobesity and antidiabetic activity. *Mol Endocrinol*. 2002;16(11):2628–2644.
20. Schopfer FJ, et al. Covalent peroxisome proliferator-activated receptor gamma adduction by nitro-fatty acids: selective ligand activity and anti-diabetic signaling actions. *J Biol Chem*. 2010;285(16):12321–12333.
21. Jansson EA, et al. The Wnt/beta-catenin signaling pathway targets PPARgamma activity in colon cancer cells. *Proc Natl Acad Sci U S A*. 2005; 102(5):1460–1465.
22. Liu J, Wang H, Zuo Y, Farmer SR. Functional interaction between peroxisome proliferator-activated receptor gamma and beta-catenin. *Mol Cell Biol*. 2006; 26(15):5827–5837.
23. Marx N, Bourcier T, Sukhova GK, Libby P, Plutzky J. PPARgamma activation in human endothelial cells increases plasminogen activator inhibitor type-1 expression: PPARgamma as a potential mediator in vascular disease. *Arterioscler Thromb Vasc Biol*. 1999;19(3):546–551.
24. Hay DL, Walker CS, Poyner DR. Adrenomedullin

and calcitonin gene-related peptide receptors in endocrine-related cancers: opportunities and challenges. *Endocr Relat Cancer*. 2010;18(1):C1–C14.
25. Kasai A, et al. Apelin is a novel angiogenic factor in retinal endothelial cells. *Biochem Biophys Res Commun*. 2004;325(2):395–400.
26. Watanabe K, et al. Vasohibin as an endothelium-derived negative feedback regulator of angiogenesis. *J Clin Invest*. 2004;114(7):898–907.
27. Goetze JP, et al. Apelin: a new plasma marker of cardiopulmonary disease. *Regul Pept*. 2006; 133(1–3):134–138.
28. Falcao-Pires I, et al. Apelin decreases myocardial injury and improves right ventricular function in monocrotaline-induced pulmonary hypertension. *Am J Physiol Heart Circ Physiol*. 2009;296(6):H2007–H2014.
29. Chandra SM, et al. Disruption of the apelin-APJ system worsens hypoxia-induced pulmonary hypertension. *Arterioscler Thromb Vasc Biol*. 2010; 31(4):814–820.
30. Lee DK, et al. Characterization of apelin, the ligand for the APJ receptor. *J Neurochem*. 2000;74(1):34–41.
31. Sorli SC, van den Berghe L, Masri B, Knibiehler B, Audigier Y. Therapeutic potential of interfering with apelin signalling. *Drug Discov Today*. 2006;11(23–24):1100–1106.
32. Lea MA, Sura M, Desbordes C. Inhibition of cell proliferation by potential peroxisome proliferator-activated receptor (PPAR) gamma agonists and antagonists. *Anticancer Res*. 2004;24(5A):2765–2771.
33. Nissen SE, Wolski K. Effect of rosiglitazone on the risk of myocardial infarction and death from cardiovascular causes. *N Engl J Med*. 2007; 356(24):2457–2471.
34. Michaelson J. Thiazolidinedione associated volume overload and pulmonary hypertension. *Ther Adv Cardiovasc Dis*. 2008;2(6):435–438.
35. Baker PR, et al. Fatty acid transduction of nitric oxide signaling: multiple nitrated unsaturated fatty acid derivatives exist in human blood and urine and serve as endogenous peroxisome proliferator-activated receptor ligands. *J Biol Chem*. 2005;280(51):42464–42475.
36. Freeman BA, Baker PR, Schopfer FJ, Woodcock SR, Napolitano A, d'Ischia M. Nitro-fatty acid formation and signaling. *J Biol Chem*. 2008; 283(23):15515–15519.
37. Li Y, et al. Molecular recognition of nitrated fatty acids by PPAR gamma. *Nat Struct Mol Biol*. 2008; 15(8):865–867.
38. Perez VA, et al. BMP promotes motility and represses growth of smooth muscle cells by activation of tandem Wnt pathways. *J Cell Biol*. 2011;192(1):171–188.
39. Mulholland DJ, Dedhar S, Coetzee GA, Nelson CC. Interaction of nuclear receptors with the Wnt/beta-catenin/Tcf signaling axis: Wnt you like to know? *Endocr Rev*. 2005;26(7):898–915.
40. Szokodi I, et al. Apelin, the novel endogenous ligand of the orphan receptor APJ, regulates cardiac contractility. *Circ Res*. 2002;91(5):434–440.
41. Tatemoto K, et al. Isolation and characterization of a novel endogenous peptide ligand for the human APJ receptor. *Biochem Biophys Res Commun*. 1998; 251(2):471–476.
42. Sakao S, Taraseviciene-Stewart L, Wood K, Cool CD, Voelkel NF. Apoptosis of pulmonary microvascular endothelial cells stimulates vascular smooth muscle cell growth. *Am J Physiol Lung Cell Mol Physiol*. 2006;291(3):L362–L368.
43. Hashimoto T, et al. Requirement of apelin-apelin receptor system for oxidative stress-linked atherosclerosis. *Am J Pathol*. 2007;171(5):1705–1712.
44. Chun HJ, et al. Apelin signaling antagonizes Ang II effects in mouse models of atherosclerosis. *J Clin Invest*. 2008;118(10):3343–3354.
45. Charo DN, et al. Endogenous regulation of cardiovascular function by apelin-APJ. *Am J Physiol Heart Circ Physiol*. 2009;297(5):H1904–H1913.
46. Kasai A, et al. Retardation of retinal vascular development in apelin-deficient mice. *Arterioscler Thromb Vasc Biol*. 2008;28(10):1717–1722.
47. Sheikh AY, et al. In vivo genetic profiling and cellular localization of apelin reveals a hypoxia-sensitive, endothelial-centered pathway activated in ischemic heart failure. *Am J Physiol Heart Circ Physiol*. 2008;294(1):H88–H98.
48. Kleinz MJ, Davenport AP. Immunocytochemical localization of the endogenous vasoactive peptide apelin to human vascular and endocardial endothelial cells. *Regul Pept*. 2004;118(3):119–125.
49. McMurtry MS, et al. Dichloroacetate prevents and reverses pulmonary hypertension by inducing pulmonary artery smooth muscle cell apoptosis. *Circ Res*. 2004;95(8):830–840.
50. Zhao YD, et al. Microvascular regeneration in established pulmonary hypertension by angiogenic gene transfer. *Am J Respir Cell Mol Biol*. 2006;35(2):182–189.
51. Jia YX, et al. Apelin protects myocardial injury induced by isoproterenol in rats. *Regul Pept*. 2006; 133(1–3):147–154.
52. Spiekerkoetter E, et al. S100A4 and bone morphogenetic protein-2 codependently induce vascular smooth muscle cell migration via phospho-extracellular signal-regulated kinase and chloride intracellular channel 4. *Circ Res*. 2009; 105(7):639–647.
53. Tusher VG, Tibshirani R, Chu G. Significance analysis of microarrays applied to the ionizing radiation response. *Proc Natl Acad Sci U S A*. 2001; 98(9):5116–5121.